Title

Evaluation of Coupled Thermal and Hydraulic Relationships Used in Simulation of Thermally-Induced Water Flow in Unsaturated Soils

Authors

Başer, Tuğçe
McCartney, John S
Dong, Yi
et al.

Publication Date

2018-06-20

DOI

10.1061/9780784481691.037

Peer reviewed

Evaluation of Coupled Thermal and Hydraulic Relationships used in Simulation of Thermally-Induced Water Flow in Unsaturated Soils

Tuğçe Başer[1], Ph.D., S.M.ASCE; John S. McCartney[2], Ph.D., P.E., M.ASCE; Yi Dong, Ph.D., M. ASCE[3]; and Ning Lu[4], Ph.D., F.ASCE

[1]Research Associate, University of Alberta, Dept. of Civil and Environmental Engineering, 9211 - 116 Street NW Edmonton, Alberta, Canada T6G 1H9. tugce@ualberta.ca.
[2]Associate Professor, University of California San Diego, Department of Structural Engineering, 9500 Gilman Dr., La Jolla, CA 92093-0085, mccartney@ucsd.edu.
[3]Associate Professor, State Key Laboratory of Geomechanics and Geotechnical Engineering, Institute of Rock and Soil Mechanics, Chinese Academy of Sciences, Wuhan, Hubei 430071, P.R. China. ydong@whrsm.ac.cn.
[4]Professor, Colorado School of Mines, Department of Civil and Environmental Engineering, 1500 Illinois St., Golden, CO, 80401, ninglu@mines.edu.

ABSTRACT

This paper focuses on the role of coupling between the thermal and hydraulic properties of soils on simulations of the distribution in temperature and degree of saturation surrounding a geothermal heat exchanger in an unsaturated soil deposit. This information is relevant to the simulation of geothermal heat storage systems in unsaturated soil layers. The simulations involved heat transfer coupled with water flow in both liquid and vapor forms, and were performed considering the properties of sand, silt, and clay. A water table was fixed at a depth of 20 m below the extent of the heat exchanger, which means that the different soils considered have different initial hydraulic conditions along the length of the heat exchanger. After heat injection for 90 days at the same heat injection rate, the ground temperatures varied significantly with the soil type, with the clay showing the greatest changes in temperature despite having a lower thermal conductivity than the sand. The clay layer also experienced the greatest changes in degree of saturation and had the highest heat transfer due to latent heat transfer, likely because the initial degree of saturation was higher in this soil. The results indicate that a larger change in degree of saturation may occur in soils with a higher initial hydraulic conductivity.

INTRODUCTION

Recent studies have demonstrated the success of using the subsurface soil or rock as a medium for storing thermal energy collected from solar thermal panels, in which heat is transferred into the subsurface by circulation of heated fluid through a network of closely-spaced, closed-loop geothermal heat exchangers (Sibbitt et al. 2012; Baser et al. 2016a; McCartney et al. 2017). Design methodologies have been developed for geothermal heat storage systems, but they rely on the assumption of constant values of the

soil thermal properties such as the thermal conductivity and volumetric heat capacity (e.g., Claesson and Hellström 1981). It is well established that the thermal properties of unsaturated soils vary with degree of saturation, and a range of different models have been developed to quantify these trends (Dong et al. 2015). Wu et al. (2015) found that using constant thermal conductivity values when simulating the response of geothermal heat exchangers in unsaturated soil deposits can lead to significant errors in the calculated heat transfer rates. These errors may lead to oversizing of the network of geothermal heat exchangers, potentially leading to greater installation costs. The hydraulic properties of soils and the temperature-dependency of the fluid properties can have an influence on the heat transfer processes from geothermal heat exchangers. For example, Catolico et al. (2016) found that saturated soils with higher hydraulic conductivity will experience convective heat transfer due to buoyancy-driven water flow away from the heat exchangers. Therefore, an understanding of coupled thermo-hydraulic relationships and temperature effects on the properties of liquid water and moist air are essential to accurately simulate the simultaneous heat transfer and water flow in unsaturated soils. This paper focuses on numerical thermal response of a single borehole heat exchanger surrounded by different types of unsaturated soils with different ranges of thermo-hydraulic properties (sand, silt, and clay). To characterize the impact of coupled thermo-hydraulic constitutive relationships on the thermal response of unsaturated soil layers surrounding a geothermal heat exchanger, three-dimensional solutions to the coupled heat transfer and water flow model considering enhanced vapor diffusion and nonequilibrium phase change developed by Smits et al. (2011) and extended by Moradi et al. (2016) was used in this study. Although this model is more complex than previous models such as that of Philip and de Vries (1957), Smits et al. (2011) found that it better captured the results from an experiment involving evaporation from a heated soil column due to the separate consideration of liquid water and water vapor.

BACKGROUND

Transfer and Transport Mechanisms

When an unsaturated soil is heated, heat transfer may occur due to conduction, convection, and latent heat transfer associated with water phase change (Philip and de Vries 1957; Smits et al. 2011). Conduction in unsaturated soils depends on the degree of saturation, with heat conduction through dry soils being greater than that through air but less than through water, and heat conduction through saturated soils being greater than that through water but less than that through the soil minerals (Dong et al. 2015). Convection in unsaturated soils depends on the presence of hydraulic gradients causing advective movement of the pore fluids, as well as due to temperature effects on the fluid properties that result in additional drivers for fluid flow. Temperature has been shown to have major effects on the density and viscosity of liquid water and moist air, as well as other key parameters such as the equilibrium vapor pressure, relative humidity at equilibrium, water vapor diffusion coefficient in air, surface tension, and latent heat of vaporization (Smits et al. 2011). Latent heat transfer depends on the initial degree of saturation of the soil. More phase change can occur in soils with greater initial degrees of

saturation due to the greater availability of liquid water in the pores to change phase, but greater amounts of enhanced vapor diffusion will occur when the initial degree of saturation is lower. For a silt, McCartney and Baser (2017) found that greater changes in degree of saturation occurred for greater initial degrees of saturation due to the combination of the different mecahnisms of thermally-induced water flow, but this may not be a general observation for all soils.

Underlying Assumptions in the Numerical Model

In the numerical model formulation, the following assumptions are made: (1) soil framework is homogeneous, isotropic, and non-deformable, (2) pore fluids are incompressible, (3) fluid phases are immiscible, (4) hysteresis of the constitutive relationship is not considered, (5) total gas phase is assumed to be binary mixture of dry air and vapor and complies with the ideal gas law.

Formulation

To investigate the role of the coupled thermo-hydraulic relationships on thermal response of borehole heat exchangers, a coupled heat transfer and water flow model which accounts for vapor flow is developed. A two-phase flow model can be used to solve for liquid water and total gas phase in unsaturated soils, as follows (Bear 1972):

$$nS_{rw}\frac{\partial \rho_w}{\partial t}+n\,\rho_w\frac{dS_{rw}}{dP_c}\frac{\partial P_c}{\partial t}+\nabla\cdot\left[\rho_w\left(-\frac{k_{rw}\kappa}{\mu_w}\right)\nabla\left(P_w+\rho_w gz\right)\right]=¿-R_{gw}¿ \tag{1}$$

$$nS_{rg}\frac{\partial \rho_g}{\partial t}+n\,\rho_g\frac{dS_{rg}}{dP_c}\frac{\partial P_c}{\partial t}+\nabla\cdot\left[\rho_g\left(-\frac{k_{rg}\kappa}{\mu_g}\right)\nabla\left(P_g+\rho_g gz\right)\right]=¿R_{gw}¿ \tag{2}$$

where n is the porosity (m^3/m^3), S_{rw} and S_{rg} are the degrees of water and gas saturation (m^3/m^3), respectively, ρ_w and ρ_g are the temperature-dependent densities of water and gas (kg/m^3), respectively , t is time (s), $P_c=P_w-P_g$ is the capillary pressure (Pa), P_w is the pore water pressure (Pa), P_g is the pore gas pressure (Pa), k_{rw} and k_{rg} are the relative permeability functions for water or gas (m/s), respectively, κ is the intrinsic permeability (m^2), μ_w and μ_g are the temperature-dependent water and gas dynamic viscosities (kg/(ms)), respectively, g is the acceleration due to gravity (m/s^2), R_{gw} is the phase change rate (kg/m^3s), and z is depth (m). The mass balance for water vapor in the gas phase can be expressed as follows:

$$n\frac{\partial\left(\rho_g S_{rg} w_v\right)}{\partial t}+\nabla\cdot\left(\rho_g u_g w_v-D_e\rho_g\nabla w_v\right)=R_{gw} \tag{3}$$

where w_v is the mass fraction of water vapor in the gas phase (kg/kg) and D_e is the effective diffusion coefficient (m^2/s) is equal to the product of the vapor diffusion coefficient in air with tortuosity, as follows (Campbell 1985):

$$D_e = D_v \tau \tag{4}$$

where D_v is the binary diffusion coefficient (m^2/s) and τ is the tortuosity which is the available space in the pores for fluid to flow. The Millington and Quirk (1961) tortuosity model was used in this study, and is given as follows:

$$\tau = \left(n^{1/3}\right)\left(S_{rg^{7/3}}\right)\eta \tag{5}$$

where η is the vapor enhancement factor defined by Cass et al. (1984), as follows:

$$\eta = a + 3S_{rw} - (a-1)\exp\left\{-\left[\left(1+\frac{2.6}{\sqrt{f_c}}\right)S_{rw}\right]^3\right\} \tag{6}$$

where a is an empirical constant to be determined experimentally that changes the magnitude of the enhancement factor and f_c is the mass fraction of clay. A method based on the difference between the vapor pressure in air and the equilibrium pressure at the water-gas interface was used (Bixler 1985), where the phase change rate is defined as:

$$R_{gw} = \left(\frac{bS_{rw}RT}{M_w}\right)(\rho_{veq} - \rho_v) \tag{7}$$

where b is an empirical fitting parameter (s/m^2) that needs to be determined experimentally, R is universal gas constant (J/molK), ρ_{veq} is the temperature-dependent equilibrium vapor density (kg/m^3), T is the temperature (K), $\rho_v = \rho_g w_v$ is the actual vapor density (kg/m^3), and M_w is the molecular weight of water. The heat equation that includes conduction and convection is derived from Fourier's law and the first law of thermodynamics, as follows:

$$(\rho C_p)\frac{\partial T}{\partial t} + \nabla .\left((\rho_w C_{pw})u_w T + (\rho_g C_{pg})u_g T - (\lambda \nabla T)\right) = ¿ - L_w R_{gw} + Q ¿ \tag{8}$$

where ρ is the total density of soil (kg/m^3), C_p is the specific heat of soil (J/kgK), C_{pw} is the specific heat capacity of water (J/kgK), C_{pg} is the specific heat capacity of gas (J/kgK), λ is the thermal conductivity (W/mK), L_w is the latent heat of water vaporization (J/kg), u_w is the water velocity (m/s), u_g is the gas velocity (m/s), and Q is a heat source (W/m^3).

ANALYSIS

Equations 1, 2, 3, and 8 were solved simultaneously using COMSOL Multiphysics version 5.2a. Simulations were performed to predict the distributions in temperature and

degree of saturation around a geothermal heat exchanger in sand, silt, and clay layers to understand the impacts of soil type and initial degree of saturation on the subsurface heating and cooling response. The geothermal borehole heat exchanger investigated in this study has a length of 15 m and a radius of 0.04 m, and is embedded in a 3D soil domain. Although the problem under investigation in this study is axisymmetric, a one-quarter domain was used because this simplifies the extension of this model to simulations with more geothermal borehole heat exchangers in the future. The domain along with the hydraulic and thermal boundary conditions for the models is shown in Figure 1. Because it is common in practice to include a surficial hydraulic barrier to prevent vapor loss to the atmosphere, for liquid water and gas flow, no mass flux was assumed for all boundaries except the bottom boundary. A constant water pressure equal to zero was applied at the bottom boundary to represent the water table. For heat transfer, a constant temperature representing an average subsurface soil temperature of 21 °C was applied at the bottom boundary. A constant heat flux of 100 W/m^2 was applied to the outer boundary of the heat exchanger during the heating period. The initial ambient temperature of the domain was assumed to be a function of depth, since ambient surface temperature fluctuations may influence the temperature profiles during heat injection even with the presence of an insulation layer (Başer et al. 2016c). This influence may extend to a depth of approximately 9 m from the surface, below which the soil temperature can be assumed to be constant and equal to the average ambient air temperature. A water table was assumed to be at a depth of 20 m (the bottom of the domain). This depth was selected so that the soil along the length of the heat source will be unsaturated, with initial degrees of saturation ranging from 1.00 to 0.09 depending on the height from the water table and soil type. For a water table at a depth of 20 m, the initial degree of saturation ranges from 0.12-0.09 in the sand layer, while these values for the silt and clay layers are 0.55-0.26 and 0.80-0.61, respectively. Although this choice of initial conditions leads to a complex comparison between the soil types, it is representative of typical initial conditions encountered in nature.

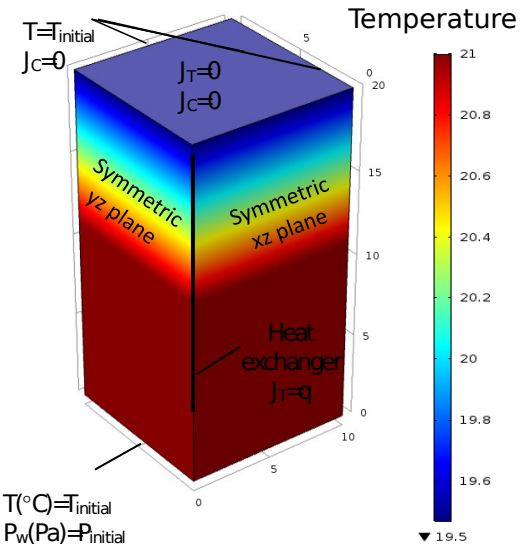

Figure 1. Initial and boundary conditions on the quarter domain for a field-scale

geothermal heat exchanger (J_T and J_C are heat and mass fluxes, distances in meters)

Four fundamental constitutive relationships, the soil water retention curve (SWRC) (van Genuchten 1980), hydraulic conductivity function (HCF) (van Genuchten 1980), thermal conductivity function (TCF) (Lu and Dong 2015), and volumetric heat capacity function (VHCF) (Baser et al. 2016b) are used in solving the governing equations for heat transfer and water flow in unsaturated soils. The SWRC, HCF, TCF, and VHCF for three soils obtained from Lu and Dong (2015) are shown in Figures 2(a), 2(b), 2(c), and 2(d), respectively, for sand (Accusand 40/50), silt (Bonny silt), and clay (reconstituted Denver claystone). The equations for the four thermo-hydraulic relationships are shown in Figure 2, and the parameters for the soils used in the analyses were measured by Lu and Dong (2015) and are summarized in Table 1. Lu and Dong (2015) performed a statistical evaluation of the parameters of the TCF and found that they were closely related to the SWRC parameters, confirming coupling between these relationships. Empirical fitting parameters *a* and *b* in Table 1 were selected from calibration data reported by Smits et al. (2011) for sand and by McCartney and Baser (2017) for silt. The values of *a* and *b* were assumed for clay based on the observed trend in these parameters from sand to silt.

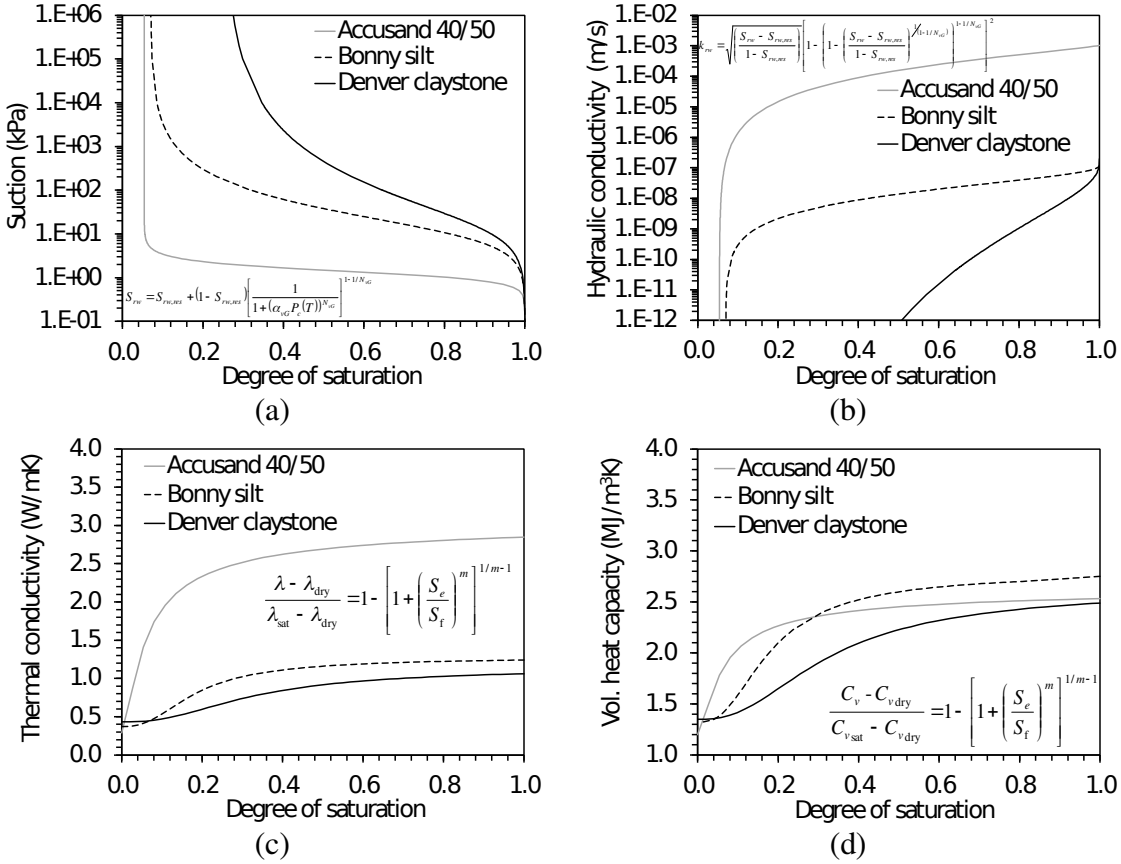

Figure 2. Constitutive relationships: (a) SWRC; (b) HCF; (c) TCF; (d) VHCF

Table 1: Details of the thermal and hydraulic parameters of the soils investigated

Property	Accusand 40/50	Bonny silt	Denver claystone
n, Porosity	0.37	0.43	0.51
λ_{sat} (W/mK), thermal conductivity of saturated soil	3.10	1.27	1.15
λ_{dry} (W/mK), thermal conductivity of dry soil	0.29	0.37	0.43
$C_{v,sat}$ (MJ/m^{3}K), volumetric heat capacity of saturated soil	2.5	2.7	2.4
$C_{v,dry}$ (MJ/m^{3}K), volumetric heat capacity of dry soil	1.2	1.3	1.3
K_{sat} (m/s), hydraulic conductivity of saturated soil	1.0×10^{-3}	5.4×10^{-7}	2.2×10^{-7}
α_{vG} (1/kPa), SWRC parameter	0.77	0.088	0.071
N_{vG}, SWRC parameter	4.10	1.58	1.32
θ_r, residual volumetric water content	0.02	0.03	0.13
m, TCF fitting parameter	1.70	2.62	2.52
S_f, TCF fitting parameter	0.032	0.145	0.25
a, enhanced vapor diffusion coefficient	18.2	30	40
b, phase change rate coefficient	2.1×10^{-5}	5.0×10^{-7}	5.0×10^{-8}

RESULTS

The sand, silt, and clay layers were subjected to a 90-day heating period followed by a 60-day cooling period. These heating and cooling periods represent a typical heat injection and cooling periods in a geothermal heat storage system. Distributions in ground temperatures in the y-z plane (width of 10 m and depth of 20 m) at an x coordinate of 0 m at the end of heating are shown in Figures 3(a-c) for the three soils. The highest temperature of 75 °C was observed 3 m from the surface at the borehole wall in the clay layer while the lowest temperature of 42 °C with a uniform distribution was observed in the sand layer, despite the sand having a much greater thermal conductivity than the clay. During heating, the greatest changes in temperature were within 1 m of the borehole wall for the three soils. After 60 days of cooling, the temperature was observed to be more distributed in the soil layers, with the highest retained temperature of 26 °C in the clay layer at the borehole wall. The retained temperatures in the silt and sand soil layers were 25 and 24 °C, respectively.

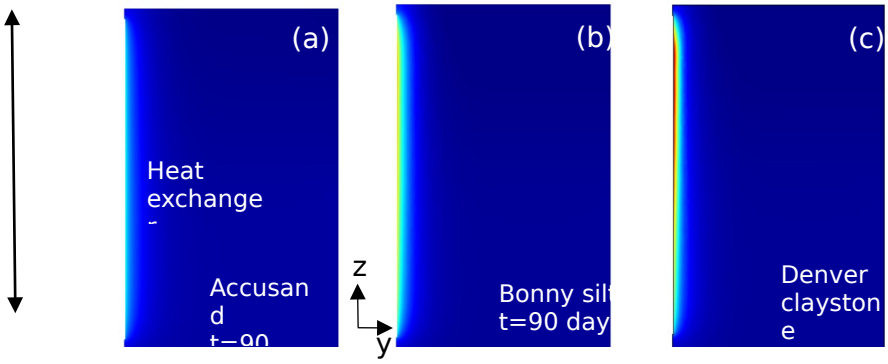

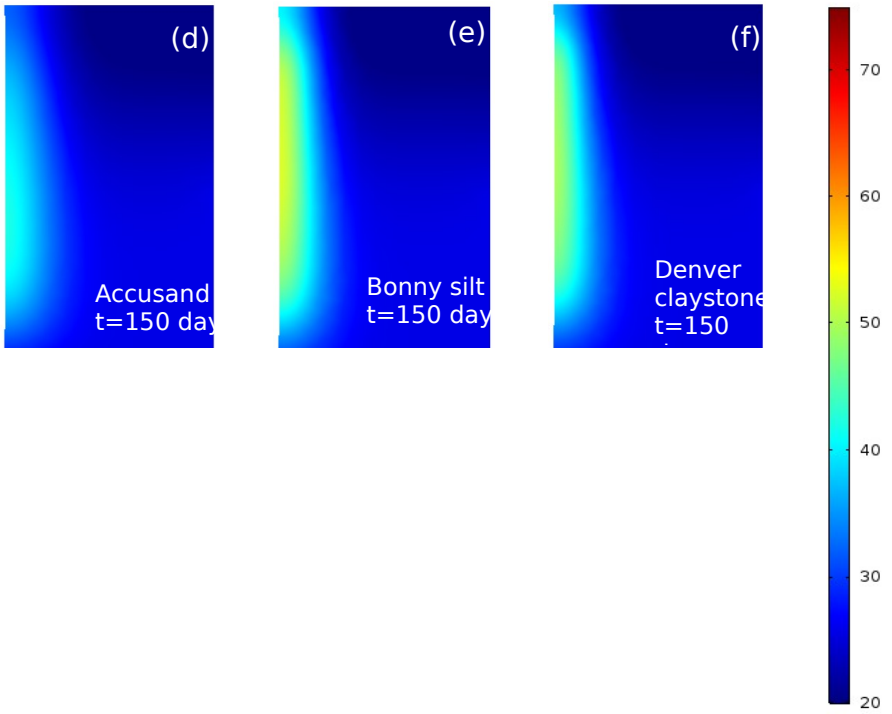

Figure 3. Ground temperatures (°C) in different soil layers after: (a, b, c) 90 days of heating and (d, e, f) 60 subsequent days of cooling

The corresponding distributions in degree of saturation at the ends of the heating and cooling periods are plotted in Figure 4. Since the initial degree of saturation of the sand layer along the length of the heat exchanger is very close to its residual value, there was only a minor change in degree of saturation of 0.07 (Figure 4a). The changes in degree of saturation were higher in the silt and clay layers, with maximum decreases in the degree of saturation after the heating period of 0.13 and 0.36, as shown in Figures 4(b) and 4(c), respectively. These changes are attributed to the different initial degrees of saturation, as well as to the effects of enhanced vapor diffusion and phase change in these soils. An interesting observation is that at the end of the cooling period, the changes in degree of saturation in the silt layer did not fully recover (i.e., permanent drying near the heat exchanger). However, the changes in degree of saturation in the clay layer were observed to recover somewhat as shown in Figure 4(f). This may be due to the continuity of the liquid water phase in the clay layer but not in the silt layer. The lower temperatures after cooling for the sand and silt observed in Figure 3 are due to both the lower temperatures observed during heating for these soils as well as due to the different changes in the thermal properties of the soils during heating associated with the decreases in degree of saturation. For instance, a degree of saturation of 0.1 (observed near the heat exchanger in all three soils) is associated with thermal conductivity values of 2.21 W/mK for sand, 0.97 W/mK for silt and 0.56 W/mK for clay.

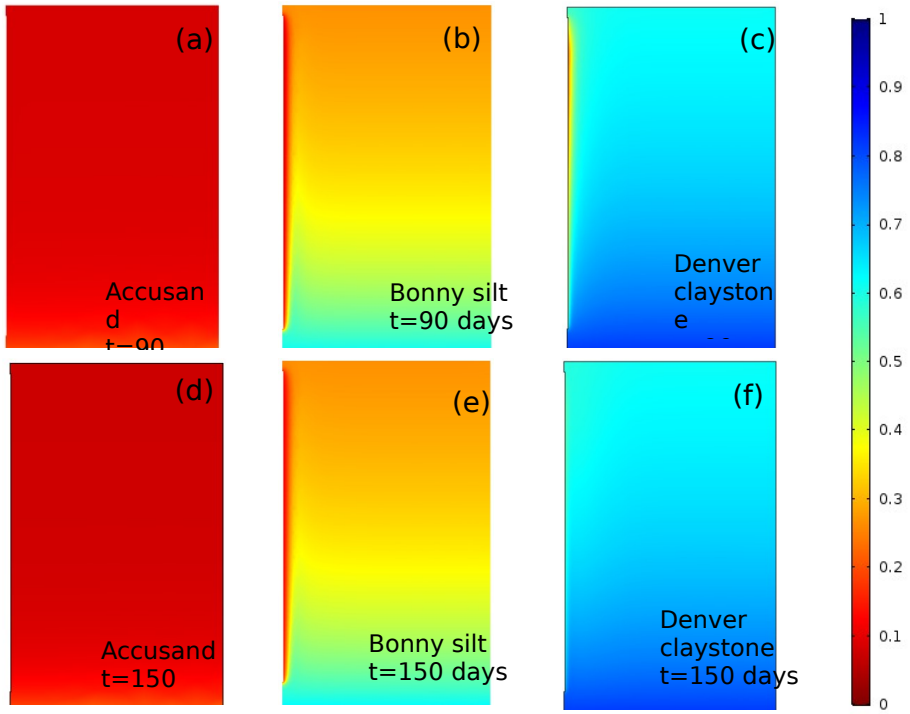

Figure 4. Degrees of saturation (m^3/m^3) in different soil layers after: (a, b, c) 90 days of heating and (d, e, f) 60 subsequent days of cooling

The role of latent heat transfer was assessed by showing the distributions in the phase change rates (i.e., the term $L_w R_{gw}$ in Eq. 8) for the different soils in Figure 5 at the ends of the heating and cooling periods. The highest amount of latent heat transfer at the end of the heating period was observed in the clay layer with the value of 1140 J/m^3. This value was 176 and 25 J/m^3 for the silt and sand layers, respectively. Much lower values were observed during cooling due to the lower gradient. Although the phase change rate is affected by the temperature of the soil layer according to Eq. 7, previous studies reported that effect of the soil temperature on latent heat transfer is not significant (e.g., Moradi et al. 2016). Instead, the phase change rate primarily depends on the combined effects of the degree of saturation and vapor concentration (e.g., Moradi et al. 2016). Specifically, more phase change is observed in soils with higher initial degrees of saturation as there is a greater amount of liquid water available to evaporate. On the other hand, higher initial degrees of saturation can hinder vapor transport and consequently latent heat transfer.

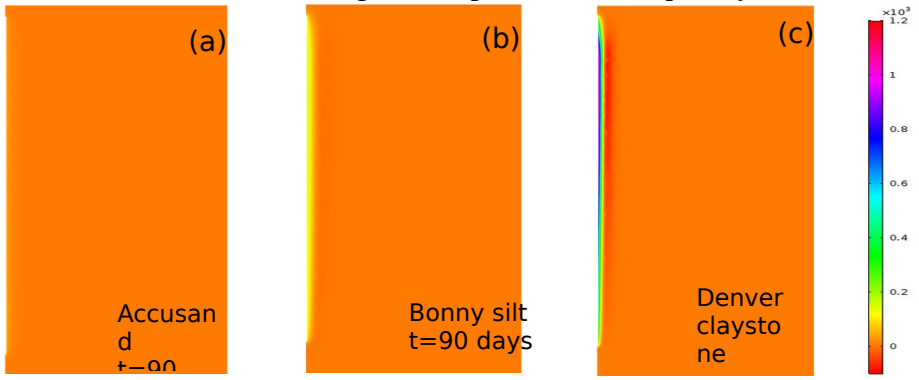

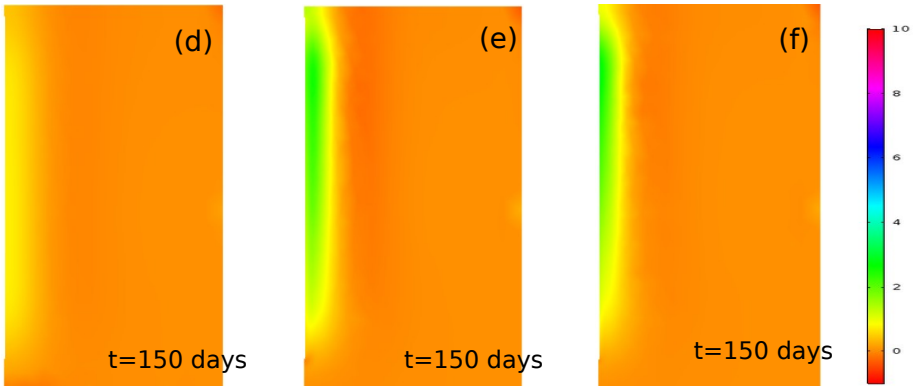

Figure 5. Latent heat transfer (J/m^3) due to water phase change in different soil layers after: (a, b, c) 90 days of heating and (d, e, f) 60 subsequent days of cooling

CONCLUSIONS

This study investigated the coupled heat transfer and water flow from a geothermal heat exchanger embedded in three different soil layers (sand, silt, and clay) having different coupled thermo-hydraulic properties. The soil layers were subjected to a period of sustained heating followed by a cooling period. A general observation from the spatial distributions in temperature and degree of saturation is that the soil properties and the corresponding initial hydrological setting play major roles in the coupled heat transfer and water flow process. Although the difference in temperature after the cooling period for the different soil layers was not significant for the example considered (1-2 °C), this change in temperature can represent a significant amount of energy. However, the clay layer experienced the greatest decrease in degree of saturation during heating, so it showed the slowest decrease in temperature with time during cooling. The clay layer also experienced the greatest recovery of the decrease in degree of saturation during cooling. The highest values of latent heat transfer due to phase change were observed in clay due to a combination of higher initial degree of saturation but high enhanced vapor diffusion. The lowest latent heat transfer was observed in the sand as it was at nearly residual saturation.

ACKNOWLEDGEMENTS

Funding from National Science Foundation (NSF 1230237) is much appreciated. The opinions are those of the authors alone and do not reflect those of the sponsor.

REFERENCES

Başer, T., Lu, N., and McCartney, J.S. (2016a). “Operational response of a soil-borehole thermal energy storage system.” ASCE Journal of Geotechnical and Geoenvironmental Engineering. 142(4), 04015097-1-12. 10.1061/(ASCE)GT.1943-5606.0001432.

Başer, T., Dong, Y., Lu, N., and McCartney, J.S. (2016b). “Role of considering non-constant soil thermal parameters in the simulation of geothermal heat storage systems in the vadose zone.” Proc. 8th Asian Young Geotechnical Engineers Conf. 137-142.

Başer, T., Dong, Y., and McCartney, J.S. (2016c). “Heat content in soil-borehole thermal energy systems in the vadose zone.” Proc. Int Conf. on Energy Geotech. Kiel.195-202.
Bear, J. (1972). Dynamics of Fluids in Porous Media. Dover, Mineola, N. Y., 764 p.
Bixler, N.E. (1985). NORIA: A Finite Element Computer Program for Analyzing Water, Vapor, Air and Energy Transport in Porous Media. SAND84-2057, Sandia National Laboratories, Albuquerque, NM.
Campbell, G.S. (1985). Soil Physics with BASIC: Transport Models for Soil–Plant Systems. Elsevier, New York.
Cass, A., Campbell, G.S., and Jones. T.L. (1984.) “Enhancement of thermal water vapor diffusion in soil.” Soil Science Society of America. 48(1), 25–32.
Catolico, N., Ge, S., and McCartney, J.S. (2016). “Numerical modeling of a soil-borehole thermal energy storage system.” Vadose Zone J. 15(1), 1-17.
Claesson, J. and Hellström, G. (1981). “Model studies of duct storage systems.” New Energy Conservation Tech. and their Commercialization. Springer, Berlin. 762-778.
Dong, Y., McCartney, J.S. and Lu, N. (2015). “Critical review of thermal conductivity models for unsaturated soils.” Geotechnical and Geological Eng. 33(2), 207-221.
Lu, N. and Dong, Y. (2015). “A closed form equation for thermal conductivity of unsaturated soils at room temperature.” J. Geotech. Geoenv. Eng. 141(6), 04015016.
McCartney, J.S. and Baser, T. (2017). “Role of coupled processes in thermal energy storage in the vadose zone.” 2nd Int. Symp. on Coupled Phen. in Env. Geotech. Leeds, UK. 1-6.
Millington, R.J., and Quirk, J.M. (1961). “Permeability of porous solids.” Trans. Faraday Soc. 57, 1200–1207.
Moradi, A.M., Smits, K., Lu, N., and McCartney, J.S. (2016). “Heat transfer in unsaturated soil with application to borehole thermal energy storage.” Vadose Zone J. 15(10), 1-17.
Philip, J.R., and de Vries, D.A. (1957). “Moisture movement in porous materials under temperature gradients.” Trans. Amer. Geophys. Union 38:222–232.
Sibbitt, B., McClenahan, D., Djebbar, R., Thornton, J., Wong, B., Carriere, J., Kokko, J. (2012). “The performance of a high solar fraction seasonal storage district heating system - Five years of operation.” Energy Procedia. 30, 856-865.
Smits, K.M., Cihan, A., Sakaki, T., and Illangasekare, T.H. (2011). “Evaporation from soils under thermal boundary conditions: Experimental and modeling investigation to compare equilibrium and nonequilibrium-based approaches.” Water. Resour. Res. 47, W05540, doi:10.1029/2010WR009533.
van Genuchten, M.T. (1980). “A closed-form equation for predicting the hydraulic conductivity of unsaturated soils.” Soil Sci. Soc. Am. J., 44(5), 892–898.
Wu, R., Tinjum, J.M. and Likos, W.J. (2015). “Coupled thermal conductivity dryout curve and soil–water characteristic curve in modeling of shallow horizontal geothermal ground loops”. Geotech. and Geol. Engineering. 33(2), 193-205.